Comprehensive Evaluation and Analysis of the Salinity Stress Response Mechanisms Based on Transcriptome and Metabolome of *Staphylococcus Aureus*

Ying Feng
Ningbo University
Dizhou Gu
Tonghua Normal University
Ziyan Wang
Ningbo University
Chenyang Lu
Ningbo University
Jingfeng Fan
National Marine Environmental Monitoring Center
Jun Zhou
Ningbo University
Rixin Wang
Ningbo University
Xiurong Su (suxiurong_public@163.com)
Ningbo University https://orcid.org/0000-0003-2336-191X

Research Article

Keywords: Staphylococcus aureus, salinity stress, transcriptome, metabolome

Posted Date: June 30th, 2021

DOI: https://doi.org/10.21203/rs.3.rs-641989/v1

Version of Record: A version of this preprint was published at Archives of Microbiology on December 18th, 2021. See the published version at https://doi.org/10.1007/s00203-021-02624-9.

Abstract

Staphylococcus aureus possesses an extraordinary ability to deal with a wide range of osmotic pressure. To performed transcriptomic and metabolomic analyses on the potential mechanism of gradient salinity stress adaptation in *S. aureus* ZS01. The results revealed that CPS biosynthetic protein genes were candidate target genes for directly regulating the phenotypic changes of biofilm. Inositol phosphate metabolism was downregulated to reduce the conversion of functional molecules. Gluconeogenesis pathway was downregulated to reduce the production of endogenous glucose. Pyruvate metabolism pathway was upregulated to promote the accumulation of succinate. TCA cycle metabolism pathway was downregulated to reduce unnecessary energy loss. These self-protection mechanisms can protect cells from hypertonic environments, and help them focus on survival. In addition, we identified 10 hub genes. The findings will aid in the prevention and treatment strategies of *S. aureus* infections.

Background

Staphylococcus aureus is an important opportunistic pathogen, which is highly resistant to osmotic stress (Schuster et al., 2016). *S. aureus* strains can generate a large scale of extracellular toxic proteins while growing or occurring in food, resulting in the outbreaks of staphylococcal food poisoning (SFP) in humans and animals (Alibayov et al., 2014). SFP is a worldwide public health problem, mainly caused by its enterotoxin, hemolysin, and leukotoxin (Loir et al., 2003). Besides, *S. aureus* can adapt and survive in harsh environments, such as drought, cold, and salinity stress (Argudín et al., 2010; Sergelidis et al., 2015). Moreover, it has a strong tolerance for many common bacteriostatic methods, and SFP accounts for a high proportion of bacterial food poisoning (Fischer et al., 2009). Therefore, research on *S. aureus* has become an important research area in the field of food safety (Xu et al., 2019).

S. aureus is considered the main pathogenic bacteria in aquatic product processing. Traditional aquatic product processing uses high-salted pickling methods to inhibit the growth of microorganisms in aquatic products, and thus prevent corruption in long-term preservation (Fuentes et al., 2010). However, the existing reports are seriously and increasingly concerned about the prevention and treatment of drug-resistant bacteria, which distracts attention from exploring the fundamental mechanism of conferring tolerance to salinity fluctuations (Wong et al., 2019; Ai et al., 2020). Therefore, the molecular mechanism of *S. aureus* for the tolerance of extremely high salt stress was studied, and its tolerance to high salt stress was weakened in a targeted way to enhance the inhibitory effect in aquatic products. The control methods of *S. aureus* are important research directions in the field of aquatic product processing, and have practical significance for the diagnosis of diseases (Price-Whelan et al., 2013). Therefore, we studied the molecular mechanism underlying the response of *S. aureus* ZS01 to extremely high salt stress. A targeted weakening of its tolerance to high salt stress can be developed as a new therapy other than antibiotics.

Generally, osmotic stress often has a great effect on the structure, chemistry, and physiology of a bacterial cell. According to previous studies on bacteria response to salinity stress, biofilm assays

showed a positive correlation between biofilm formation and increased concentration of NaCl (Beckingsale and Thomas, 2008). Islam et al. demonstrated that the addition of NaCl increased the production of polysaccharide intercellular adhesin (PIA) to induce changes in biofilm (Islam N 2015). There have been several studies on osmoregulation in *S. aureus* (Graham and Wilkinson, 1992; Cebrián et al., 2015), and choline, glycine betaine, L-proline, and taurine have demonstrated osmotic protective effect (Vijaranakul et al., 1995). The accumulation of permeating agents can effectively help bacteria to survive in a hyperosmolar environment. For example, *Listeria monocytogenes* respond to a hyperosmolar environment by transporting proteins to absorb osmotic protectants; *Bacillus subtilis* osmotically regulates by the synthesis of betaine (Boch et al., 1994; Angelidis and Smith, 2003). It has been reported that *Enterococcus faecalis* can reduce the metabolism of carbohydrates and amino acids, and increase the synthesis of nucleotide to adapt alkaline stress (Ran et al., 2015b). There are many reports about the cellular and signaling molecular responses of bacteria to osmotic stress. *Escherichia coli* increased the expression of channel proteins through the EnvZ/OmpR two-component regulatory system to increase tolerance to hyperosmotic environments (Oshima et al., 2002). In *Streptococcus mutans*, ATP-binding cassette (ABC) transporters act as sugar metabolism transporters to resist environmental stress (Nagayama et al., 2014).

In recent years, omics research has predominantly been used to explore these biological phenomena. It mainly relies on the rapid development of high-throughput sequencing technology (Xin et al., 2019). The application of these platforms makes outstanding contributions to in-depth research on the occurrence of the mechanisms. With transcriptomics data as the research background, Guan et al. evaluated the role of the *afap* 1 in oxidative stress and aflatoxin synthesis (Guan et al., 2019). Kim et al. explained the thermotolerant mechanism of *E. coli* by using transcriptome and metabolome analyses (Kim et al., 2020). In this study, transcript and metabolite datasets have been combined to reveal the response mechanism via correlation and cluster analyses, and further manifested as the connection networks between genes and metabolites. Salt-tolerant strains can evolve specific mechanisms in response to salt stress and changes. This mechanism was studied in our previous report, but it focused on the influence of DEPs at the proteomics level (Ming et al., 2019). Herein, an integrated analysis revealed more insights into the salinity stress-responsive genes, DMs, and pathway interactions than separate analysis. The screening of possible key genes and metabolites provides an opportunity for us to understand how *S. aureus* ZS01 responds to salt stress, helps us to prevent SFB infections, and develops new therapies other than antibiotics.

Materials And Methods

Bacterial strain and growth conditions

S. aureus ZS01 was separated from pickled aquatic products in Zhoushan City. Bacterial strain and growth conditions were determined using the method previously described by Ming et al (Ming et al., 2019). Briefly, *S. aureus* ZS01 was incubated for 48 hours in a broth medium supplemented with 0%, 10% and 20% NaCl, respectively.

Scanning electron microscope (SEM) analysis of morphological observation

Take 1.5mL of bacteria liquid and centrifuge at 8000×g for 4 min, discard the supernatant. The cells were processed for SEM according to the method described by Kong et al. (Kong et al., 2018). The samples were gold-coated with multifunctional sample surface treatment machine (Zhong et al., China). A Hitachi S3000N was used for the SEM image capture. The magnifications used were × 10000.

Biofilm analysis

Appropriate dilutions were made to obtain a concentration of approximately 5×10^6 CFU/mL. The solution was centrifuged at 8000×g for 2 min to collect the cells. Biofilm was stained with FITC-ConA (4°C, 30min) and PI (4°C, 15min), then imaged. Biofilm analysis was performed according to the method described by Rodriguez-Melcon et al. (Rodriguez-Melcon et al., 2019). A Zeiss LSM880 confocal laser scanning microscope (Zeiss LSM880, Germany) was used for the confocal laser scanning microscopy (CLSM) image capture. The Zen black 2.1 software is used to perform image analysis, biofilm thickness measure and export.

Total RNA isolation and transcriptome analysis

Total RNA was extracted using a commercial RNA purification kit (Invitrogen, California, USA), purity and quantity were analyzed using the Agilent2100 Bioanalyzer, and rRNA was removed using the Ribo-Zero Magnetic kit (G+/G-Bacteria) (Epicentre, Wisconsin, USA) according to the manufacturer's instruction. Sequencing was carried out on the Illumina Hiseq 4000 platform for 2 ×100 bp/300 bp (Majorbio Bio-Pharm Technology Co., Ltd., Shanghai, China) (Ran et al., 2015a).

The raw sequence data (raw reads) were filtered with the Seq Prep and Sickle software to obtain clean data. The Q20, Q30, GC-content, and sequence duplication levels of the clean data were calculated (Zhang et al., 2017). High quality reads from each sample were aligned to the reference genome *S. aureus* ATCC 27217 (https://www.ebi.ac.uk/ena/data/view/GCA_000597965) using the Bowtie software (Zhao et al., 2018). Fragments per kilobase of transcript per million fragments represented the expression values of predicted *S. aureus* transcripts (Cole et al., 2010). An adjusted FDR$\leq$ 0.05 and $|\log_2 FC| \geq 1$ were regarded as significant differentially expressed genes (DEGs). Furthermore, enrichment analysis of the DEGs was analyzed via Gene Ontology (GO) enrichment analysis and the Kyoto Encyclopedia of Genes and Genomes (KEGG) pathway analysis to obtain a detailed description. Differences with a *p*-value of $\leq$ 0.05 were used as a threshold to determine the significant enrichment.

Quantitative real-time PCR (qRT-PCR)

Ten DEGs were selected for qRT-PCR to validate our Illumina sequencing data. Total RNA was extracted using the commercial TransZol Up Plus RNA Kit (TRAN, Beijing, China) according to the manufacturer's instruction. Reverse transcription was performed using the Prime Script™ RT reagent kit (TRAN, Beijing, China). The primers were designed with the Primer Premier 5.0 software. The sequences of the primer

pairs are listed in Table S1. Rotor-Gene 6000 realtime PCR machine (Corbett, Australia) and SYBR®Premix Ex Taq™ II were used for qRT-PCR analysis. The relative gene expression was normalized internally to 16s rDNA level and quantified according to the $2^{-\Delta\Delta Ct}$ method.

Metabolite analysis

The extraction and derivatization of metabolites were performed as previously reported (Ming et al., 2018). Then gas chromatography-mass spectrometry (GC-MS) was used to analyze the metabolites. The column temperature programming was as follows: 90 ℃ held for 3 min; from 90 ℃ to 160 ℃ at 3 ℃/min, held for 0 min; from 160 ℃ to 220 ℃ at 2 ℃/min, held for 1 min; from 220 ℃ to 290 ℃ at 10 ℃/min, held for 0 min. Principal component analysis (PCA) was performed using the SIMCA-P+ver14 software (Hashim et al., 2014). Pathway analysis was performed with MetaboAnalyst 4.0 (Chong et al., 2019).

Integrated transcriptomeand metabolome analyses

Spearman correlation test was used to analyze the correlation between candidate gene expression and discriminant metabolite content. Discriminant metabolites contain aminobutanoic acid, glycolic acid, D-erythrofuranose, sebacic acid, xylitol, D-threitol, n-hexadecanoic acid, myo-Inositol, heptacosane, undecanedioic acid, L-proline, phosphoric acid, succinate, D-arabinose, and D-mannitol.

Results

High concentrations of NaCl affect morphology

In the control group, the morphology of *S. aureus* ZS01 was spherical, the surface of cell was smooth without damage or wrinkles, and the size was relatively neat (Fig. 1A). With the increase of salt concentration, there was no significant change in cell morphology in the 10% NaCl treatment group, but the number of cells was significantly lower than that in the control group (Fig. 1B). In the 20% NaCl treatment group, the cell membrane ruptured obviously, the cell contents overflowed, and some cells showed shrinkage (Fig. 1C).

From the above results, it can be seen that the morphological changes of *S. aureus* ZS01 in the 20% NaCl treatment group are more obvious than in the 10% NaCl treatment group. High salinity stress can change the permeability of cell membrane and rupture the cell membrane, leading to cell death.

High concentrations of NaCl affect biofilm formation

The distribution of the bacteria and extracellular polymeric substances (EPS) was observed from 3D views of CLSM images (Fig. 2A, 2B, and 2C). FITC-ConA can bind to cell wall polysaccharides to emit green fluorescence, and PI can penetrate bacterial cells and bind to DNA to emit red light. EPS as the main component of biofilm emits green fluorescence; bacterial DNA emits red fluorescence. With the increase of NaCl concentration, the thickness of biofilms increased and then decreased, and the

difference between adjacent groups was significant (Fig. 2D). The results show that in the concentration range of less than 10% NaCl, high concentration of NaCl contributes to the formation of biofilms. When the concentration of NaCl is higher than 10%, NaCl has an inhibitory effect on the formation of biofilm.

Transcriptomic profiling through RNA-Seq

Compared with the control group, 248 DEGs (121 upregulated and 127 downregulated) and 891 DEGs (365 upregulated and 526 downregulated) were identified in the 10% and 20% NaCl groups, respectively (Fig. 3A and Fig. 3B). Compared with the 10% NaCl group, 1063 DEGs (399 upregulated and 664 downregulated) were identified in the 20% NaCl group (Fig. 3C). Furthermore, the number of downregulated genes was higher than that of the upregulated genes in the three groups. Comparing Fig. 3A and Fig. 3B, it was found that as the salt concentration increased, more genes were mobilized to participate in the process of high salt stress.

Hierarchical cluster analysis of the DEGs was conducted using the HemI 1.0 software (Deng et al., 2014). Four expression change patterns were displayed among these DEGs with increasing concentrations of NaCl (Fig. 4). The four patterns are Pattern I (increase/increase); Pattern II (increase/decrease); Pattern III (decrease/decrease) and Pattern IV (decrease/increase) (Table S2). The numbers of DEGs that showed each pattern were 2, 80, 43, and 19, respectively. As a result, these DEGs can be considered as the candidate target genes for the direct regulation of salt stress. In addition, cluster analysis displayed that these genes affected by salt stress were abundant in some pathways related to membrane transport, redox process, metabolism, transcription factor activity, kinase activity, phosphatase activity, and stress response.

The predicted five KEGG pathways were statistically significant in the transcriptomic profiling (Table S3). For two comparison groups (0% NaCl vs 20% NaCl and 10% NaCl vs 20% NaCl), DEGs were enriched in ribosome pathways (45 genes and 51 genes). For the third comparison group (0% NaCl vs 10% NaCl), DEGs was enriched in glycolysis/gluconeogenesis metabolism (12 genes), pyruvate metabolism (12 genes), and glucagon signaling pathway (4 genes). After transcriptome enrichment analysis, we observed that the genes could be matched to the KEGG database that was mainly concentrated in energy metabolism, carbon and nitrogen metabolism.

Verification by qRT-PCR

To assess the reliability of our RNA-Seq, 10 DEGs were quantified using qRT-PCR. As shown in Fig. 5, the trend in qRT-PCR expression was in agreement with the RNA-seq expression profile. The results showed similar patterns of mRNA abundance in RNA-seq analysis and qRT-PCR. Therefore, RNA-seq results can reflect the expression of *S. aureus* transcriptome under high salt stress. Transcriptome data can be used for the analysis.

Metabolomic profiling through GC-MS

In total, 76 endogenous metabolites were identified in *S. aureus* ZS01. Then, the concentrations of 76 metabolites in these three groups were calculated based on the internal standard peak area (Table S4). Principal component analysis (PCA) is an overall presentation of the distribution of the original data for the samples. As shown in Fig. 6A, the main components of the metabolites were located in different quadrants, indicating clear discrimination among the intracellular metabolome in the three groups. To identify the metabolites affected by salt stress, orthogonal partial least squares discriminant analysis (OPLS-DA) was employed on the metabolic profiles. A total of 15 differential metabolites (DMs) were screened under VIP > 1 with $p < 0.05$ as standard. The 0% NaCl vs 10% NaCl group screened a total of ten DMs (aminobutanoic acid, glycolic acid, D-erythrofuranose, sebacic acid, xylitol, D-threitol, n-hexadecanoic acid, myo-inositol, heptacosane, and undecanedioic acid), the 10% NaCl vs 20% NaCl group screened a total of six DMs (L-proline, phosphoric acid, butanedioic acid, D-arabinose, D-mannitol, and n-hexadecanoic acid), and the 0% NaCl vs 20% NaCl group screened a total of six DMs (aminobutanoic acid, L-proline, phosphoric acid, butanedioic acid, D-arabinose, and xylitol) (Table S5).

We subjected the DMs to the pathway analysis to get the overall view of their contributions. The metabolic pathways related to salt stress responses are shown in Fig. 6B, 6C, and 6D. These pathways were mainly involved in inositol phosphate metabolism, sulfur metabolism, and TCA cycle (Table S6). Therefore, the results suggest that initiating defense (sulfur metabolism), signal response (inositol phosphate metabolism), and energy regulation (TCA cycle) are the key response pathways for *S. aureus* ZS01 to salt stress.

Integrated analysis of transcriptomeand metabolome

We combine transcriptome and metabolome data to gain insight into the regulatory network of *S. aureus* ZS01 under salt stress conditions. The transcriptome finally identified 81 related genes, and performed Spearman correlation analysis with 15 DMs. Taking a $p \leq 0.05$ as the threshold, paired regulatory relationships were plotted (Fig. 7). A total of 80 nodes that were connected in the network with 236 edges are displayed in the visualization of Cytoscape. According to the edge greater than ten genes (*antB*, *fnbA*, *gale*, *hisD*, *hisG*, *lysC*, *mnhD*, *proP*, *sdrC_D_E* and *serA*) for salinity stress response were obtained. Furthermore, all of them were present in Pattern III (decrease/decrease) expression change. Overall, the integrated multiomics analysis identified hub genes that were potentially linked to salt stress. They deserve further attention and in-depth functional study and validation for applications.

Discussion

SFP is one of the pathogenic factors in the process of aquatic production and preservation under high salt conditions all over the world (Hennekinne et al., 2012). The salt-tolerant *S. aureus* is the main factor that plagues the quality and safety of aquatic products. However, the current mechanism of *S. aureus* adaptation to salt stress is still insufficient. Therefore, this study used a variety of omics methods to clarify this mechanism in a comprehensive manner. We observed that *S. aureus* suffered a large difference in response to salinity stress. Phenotypic and physiological adaptation to environmental

conditions is driven by changes in gene regulation, metabolite accumulation, and cell signal transduction. We determined that biofilm formation, signal response, transcription factors, and energy metabolism played important roles in the salt stress defensive system of *S. aureus.*

Biofilm formation

Extracellular polymeric substances (EPS) contributed to biofilm stability and adhesion properties. Capsular polysaccharide (CPS) is the main resistant component of EPS and a major virulence factor in *S. aureus* (Lee et al., 1992; Lee et al., 1994). With the help of biofilms, bacteria exhibit more resistance to salinity stress. The change pattern of biofilm formation after salt stress is the same as the expression change Pattern II (increase/decrease) of transcriptome. In Pattern II, we found that CPS biosynthesis protein genes, such as *cap5A*, *cap5B*, *cap8C*, *capD*, *cap8F*, and *cap5D*, were candidate target genes for direct regulation of salt stress. Microbial biofilms can be used as a “protective suit” to protect microorganisms from extreme temperatures, ultraviolet radiation, extreme pH, high salinity, etc. (Yin et al., 2019). The natural ability of microorganisms to deal with harsh environments is attributed to their genetic diversity and physiological adaptability. Previous studies have indicated that bacterial EPS can help alleviate salt stress by reducing the content of sodium (Banerjee et al., 2019). So, we believe that the formation of biofilm and the production of EPS are important strategies for salt-tolerant *S. aureus* to assist in metabolism in response to salt stress. Enhanced production of EPS is the significant protection mechanism of periphytic biofilms against high concentrations of NaCl. At the same time, according to biofilm phenotype changes and differential gene expression, it can be found that the critical point of 10% NaCl is a relatively special state. These results can be used to explain the different mechanisms in *S. aureus* for tolerating ordinary high-salt and extreme high-salt.

Signal response

DM myo-inositol (VIP = 1.31) was downregulated significantly by 0.79-fold in the 10% NaCl group ($p < 0.05$) compared to the control group. At the same time, inositol phosphate metabolism has the greatest effect on this group. D-Glucose-6-phosphate is the only source of inositol ring (Raboy et al., 1996). In this study, the downregulation of fructose-1,6-bisphosphatase gene *fbp3* resulted in the decrease of glucose 6 phosphate content, which was the main reason for the downregulation of inositol content. Shao et al. proved that phosphoinositide has a synergistic effect with carbohydrate transporters, and it is closely related to ion transport (Shao et al., 2016). It can be inferred that the reduction of endogenous glucose was the main reason for the downregulation of *S. aureus* ZS01 inositol phosphate metabolism. The functions of phosphoinositide are diverse, involving processes such as stress resistance, signal response, conversion between secondary metabolites, DNA repair, and RNA transport (Hanakahi et al., 2000; Bolger et al., 2008). Inositol phosphate metabolism is complicated. It involves the conversion of various inositol phosphate molecules, which perform various functions in metabolic pathways (Fig. 8). Therefore, in this study, we speculated that *S. aureus* ZS01 reduced the conversion of functional molecules, and downregulated inositol phosphate metabolism is one of its strategies to adapt to salt stress.

Studies have shown that osmotic stress can induce the production of a variety of stress proteins, which have the functions, such as cell self-protection, nucleic acid repair, abnormal protein degradation, regulation of intracellular, and extracellular osmotic pressure (Kiran and Naomi, 2009; Vilhelmsson and Miller, 2002). General stress protein gene *dps* and universal stress protein gene *uspA-1*and *uspA-2* were upregulated significantly in the 10% NaCl group ($p < 0.01$), while downregulated significantly in the 20% NaCl group ($p < 0.01$). In *S. aureus*, both general stress response and universal stress response are widely conserved responses allowing bacteria to cope with a multitude of stressful conditions. Cold shock protein gene (*cspA*, *cspC*) and heat shock protein gene (*grpE*) showed significant up-down changes during the process of salt stress enhancement. Our results indicate that these DEGs not only respond to high and low temperature stress but also play an important role in resistance to osmotic stress. They may act as a full range of firefighters and respond to various extreme environmental changes.

Transcription factors

A higher abundance of transcription factors (TFs) as key regulators of transcription is important in *S. aureus* responses to salinity stress. Transcriptome analysis revealed that members of >30 TF families are responsive to salinity stress in candidate genes. Through the analysis of TF genes, the MarR family held the largest number, which reached 9. Evidence has shown that MarR family transcription regulators are sensors that sense changes in the environment, can bind small molecule compounds, and quickly start adaptive regulation of transcription levels, including controlling the production of virulence factors, responses to antibiotics and oxidative stress, and catabolism of aromatic compounds in the environment (Wei et al., 2007; Deochand and Grove, 2017)[24-26]. The GntR family also dominates in number. Previous studies have shown that GntR family TF combines with metabolites through allosteric effects, regulates the expression of genes, such as metabolism, drug resistance, and virulence, and responds quickly to environmental signals (Kunin and Rudy, 1991; Rigali et al., 2002). These results indicate that *S. aureus* ZS01 may be resistant to external stress by regulating the expression of certain stress tolerance genes or drug resistance genes. They turn on different regulatory systems through transcriptional regulation, so that cells can adapt to changes in the environment.

Energy metabolism

Transcriptome enrichment analysis results show that critical pathways are mainly concentrated in energy metabolism, carbon and nitrogen metabolism. Metabolome enrichment analysis results show that critical pathways are mainly concentrated in several energy metabolic pathways such as fatty acid biosynthesis, fatty acid degradation, TCA cycle, fructose and mannose metabolism. From the above results, we conclude that the regulation of energy metabolism pathways is an important strategy for *S. aureus* ZS01 to cope with salt stress.

Fructose-1,6-bisphosphatase fbp3 is one of the key rate-limiting enzymes in gluconeogenesis. It plays a major role in regulating changes in glucose content and plays an important role in sugar metabolism (Brown et al., 2009). In this study, *fbp3* was continuously downregulated with the increase of salt stress. Eventually, it leaded to downregulation of the gluconeogenesis pathway. In the process of salt stress, *S.*

aureus ZS01 reduced energy consumption by reducing the production of endogenous glucose. In the transcriptome, the pyruvate metabolism pathway fumarate hydratase *E4.2.1.2* and formate acetyltransferase *E2.3.1.54* were upregulated, leading to the upregulation of succinate content (Fig. 8). It can be found that high salt stress can promote the accumulation of succinate. The accumulation of this substance can reduce the sensitivity of the bacteria to salt stress, thereby improving the ability of the bacteria to respond to salt stress. This result has been verified in the metabolome, the relative content of DM succinate was continuously upregulated, and it participated in the TCA cycle.

ATP is the key energy substance that sustains life activities in the process of microbial metabolism. NADH or $FADH_2$ reacts with oxidized phosphoric acid via electron transfer to produce a large amount of ATP. In the two comparison groups where TCA is active, according to the transcriptome data, there are 3 common differentially expressed genes in the electron transport chain, *ssuE* (NADH-dependent FMN reductase), *ndhF* (NADH dehydrogenase subunit 5) and *sdhC* (succinate dehydrogenase cytochrome b-558 subunit) expression levels are downregulated. According to the changes in the expression levels of genes related to the electron transport chain, it is speculated that high salt has an inhibitory effect on the electron transport chain of *S. aureus* ZS01. The utilization of ATP also depends on the enzymes of the citrate cycle. As three key rate-limiting enzymes in the TCA metabolic pathway, the expression levels of *gltA* (citrate synthase), *icd* (isocitrate dehydrogenase) and *sucA* (2-oxoglutarate dehydrogenase E1 component) are downregulated. Downregulation of TCA cycle related enzymes in *S. aureus* ZS01 provides evidence for energy regulation to maintain survivable growth under salinity. The TCA overall show a low expression trend to maintain cell proliferation under high salt stress. As the salt concentration increases, the transcription of the gluconeogenesis decrease, which reduces the intracellular transport efficiency of glucose. The downregulation of these two energy metabolism pathways indicate that the cells are in a state of low energy metabolism similar to self-protection under high salt stress. In this respect, our results are consistent with previous study (Ming et al., 2019). Previous studies have shown that self-protection mechanisms can protect cells from hypertonic environments, reduce unnecessary energy loss, and help them focus on survival (Lee, 2013). Although stronger stress can hinder cell development and biomass, the life cycle is maintained, suggesting an adapted metabolism able to counteract this stress (Arbelet-Bonnin et al., 2020). We conclude that low energy metabolism was an important way to self-protect and overcome high salt stress for *S. aureus* ZS01.

Conclusion

S. aureus has an extraordinary ability to deal with a wide range of salinity changes. The exhaustive profiling of genes, metabolites, and pathways revealed important information regarding the regulatory networks underlying bacteria responses to salt stress. In this study, we confirmed that biofilm formation, signal response, transcription factors, and energy metabolism played important roles in the salt stress defensive system of *S. aureus* ZS01. Low energy metabolism is the most important self-protection strategy for *S. aureus* to cope with salinity stress. We can selectively screen potential targets for salt tolerance and pathogenicity of *S. aureus* and suppress the pathogenicity and toxicity, helping us to stop

SFB infections. Based on the analysis of omics data, this study provides new insight into selected potential targets for salt tolerance and pathogenicity of *S. aureus* in aquatic production and preservation.

Declarations

Funding

This work was supported by the National Key R&D Program of China (2019YFD0900101), the National Key R&D Program of China (Grant 2017YFC1404505), the K.C. Wong Magna Fund in Ningbo University and Scientific Research Project of Jilin Provincial Department of Education (JJKH20210531KJ).

Conflict of interest

The authors declare that they have no competing interests.

Availability of data

The raw sequencing data were deposited at the NCBI Sequence Read Archive (https://www.ncbi.nlm.nih.gov/sra) under Bioproject No. PRJNA704096.

Authors' contributions

RXW, XRS, CYL, and JZ conceived and designed the experiments. YF, WZY, DZG, and JFF carried out the experiments and data analysis. RXW, XRS, YF, and CYL were involved in drafting the manuscript. All the authors read and approved the final manuscript.

References

1. Ai X, Gao F, Yao S, Liang B, Mai J, Xiong Z, Chen X, Liang Z, Yang H, Ou Z, Gong S, Long Y, Zhou Z (2020). Prevalence, characterization, and drug resistance of *Staphylococcus aureus* in feces from pediatric patients in Guangzhou, China. Frontiers in Medicine 7: 127.
2. Alibayov B, Zdeňková K, Purkrtová S, Demnerová K, Karpíšková R. (2014). Detection of some phenotypic and genotypic characteristics of *Staphylococcus aureus* isolated from food items in the Czech Republic. Annals of Microbiology 64: 1587-1596.
3. Angelidis AS, Smith GM (2003). Three transporters mediate uptake of glycine betaine and carnitine by *Listeria monocytogenes* in response to hyperosmotic stress. Applied & Environmental Microbiology 69: 1013-1022.
4. Arbelet BD, Blasselle C, Rose PE, Redwan M, Ponnaiah M, Laurenti P, Meimoun P, Gilard F, Gakière B, Mancuso S, El-Maarouf BH, Bouteau F (2020). Metabolism regulation during salt exposure in the halophyte Cakile maritima. Environmental & Experimental Botany 177: http://www.ncbi.nlm.nih.gov/pubmed/104075.

5. Argudín MÁ, Mendoza MC, Rodicio MR (2010). Food poisoning and *Staphylococcus aureus* enterotoxins. Toxins 2: 1751-1773.
6. Banerjee A, Sarkar S, Cuadros OS, Bandopadhyay R (2019) Exopolysaccharides and Biofilms in Mitigating Salinity Stress: The Biotechnological Potential of Halophilic and Soil-Inhabiting PGPR Microorganisms. Soil Biology 56: 133-153.
7. Beckingsale, Thomas (2008). *Staphylococcus aureus*: Salt Stress, Cell Wall Deficiency, and Biofílm Formation. Durham theses: 17-64.
8. Boch J, Kempf B, Bremer E (1994). Osmoregulation in *Bacillus subtilis*: synthesis of the osmoprotectant glycine betaine from exogenously provided choline. Journal of Bacteriology 176: 5364-5371.
9. Bolger TA, Folkmann AW, Tran EJ, Wente SR (2008). The mRNA Export Factor Gle1 and Inositol Hexakisphosphate Regulate Distinct Stages of Translation. Cell 134: 624-633.
10. Brown G, Singer A, Lunin VV, Proudfoot M, Skarina T, Flick R, Kochinyan S, Sanishvili R, Joachimiak A, Edwards AM, Alexei S, Alexander F, Yakunin AK (2009). Structural and Biochemical Characterization of the Type II Fructose-1,6-bisphosphatase GlpX from *Escherichia coli* *. Journal of Biological Chemistry 284: 3784-3792.
11. Cebrián G, Arroyo C, Condón S, Manas P (2015). Osmotolerance provided by the alternative sigma factors σ(B) and rpoS to *Staphylococcus aureus* and *Escherichia coli* is solute dependent and does not result in an increased growth fitness in NaCl containing media. International Journal of Food Microbiology 214: 83-90.
12. Chong J, Wishart DS, Xia J (2019). Using MetaboAnalyst 4.0 for comprehensive and integrative metabolomics data analysis. Current Protocols in Bioinformatics 68: e86.
13. Cole T, Brian AW, Geo P, Ali M, Gordon K, Marijke VB, Steven LS, Barbara JW, Lior P (2010). Transcript assembly and quantification by RNA-Seq reveals unannotated transcripts and isoform switching during cell differentiation. Nature Biotechnology 28: 511-515.
14. Deng W, Wang Y, Liu Z, Cheng H, Xue Y (2014). HemI: A toolkit for illustrating heatmaps. PLOS ONE 9: e111988.
15. Deochand DK, Grove A (2017). MarR family transcription factors: dynamic variations on a common scaffold. Critical Reviews in Biochemistry & Molecular Biology 52: 595-613.
16. Fischer A, Francois P, Holtfreter S, Broeker B, Schrenzel J (2009). Development and evaluation of a rapid strategy to determine enterotoxin gene content in *Staphylococcus aureus*. Journal of Microbiological Methods 77: 184-190.
17. Fuentes A, Fernández-segovia I, Barat JM, Serra JA (2010). Physicochemical characterization of some smoked and marinated fish products. Journal of Food Processing & Preservation 34: 83-103.
18. Gansauge MT, Meyer M. (2013). Single-stranded DNA library preparation for the sequencing of ancient or damaged DNA. Nature Protocols 8: 737-748.
19. Graham JE, Wilkinson BJ (1992). *Staphylococcus aureus* osmoregulation: roles for choline, glycine betaine, proline, and taurine. Journal of Bacteriology 174: 2711-2716.

20. Gruszczyk J, Fleurie A, Olivares IV, Béchet E, Zanella CI, Moréra S, Meyer P, Pompidor G, Kahn R, Grangeasse C, Nessler S (2011). Structure analysis of the *Staphylococcus aureus* UDP-N-acetyl-mannosamine dehydrogenase Cap5O involved in capsular polysaccharide biosynthesis. Journal of Biological Chemistry 286: 17112-17121.
21. Guan XL, Zhao YJ, Liu X, Shang B, Xing F, Zhou L (2019). The bZIP transcription factor Afap1 mediates the oxidative stress response and aflatoxin biosynthesis in *Aspergillus flavus*. Revista Argentina de Microbiologia 51: 292-301.
22. Hanakahi LA, Bartlet JM, Chappell C, Pappin D, West SC (2000). Binding of Inositol Phosphate to DNA-PK and Stimulation of Double-Strand Break Repair. Cell 102: 721-729.
23. Hashim Z, Mukai Y, Bamba T, Fukusaki E (2014). Metabolic profiling of retrograde pathway transcription factors rtg1 and rtg3 knockout yeast. Metabolites 4: 580-598.
24. Hennekinne JA, De Buyser ML, Dragacci S (2012). *Staphylococcus aureus* and its food poisoning toxins: characterization and outbreak investigation. FEMS Microbiology Reviews 36: 815-836.
25. Islam N, Ross JM, Marten MR (2015). Proteome Analyses of *Staphylococcus aureus* Biofilm at Elevated Levels of NaCl. Clinical Microbiology 4: 219.
26. Kiran MD, Naomi B (2009). TRAP Plays a Role in Stress Response in *Staphylococcus aureus*. International Journal of Artificial Organs 32: 592-599.
27. Kumari A, Parida AK (2018). Metabolomics and network analysis reveal the potential metabolites and biological pathways involved in salinity tolerance of the halophyte *Salvadora persica*. Environmental and Experimental Botany 148: 85-99.
28. Kunin CM, Rudy J (1991). Effect of NaCl-induced osmotic stress on intracellular concentrations of glycine betaine and potassium in *Escherichia coli*, *Enterococcus faecalis*, and *staphylococci*. The Journal of Laboratory and Clinical Medicine 118: 217-224.
29. Lee CY (1992). Cloning of genes affecting capsule expression in *Staphylococcus aureus* strain M. Molecular Microbiology 6: 1515-1522.
30. Lee JC, Xu S, Albus A, Livolsi PJ (1994). Genetic analysis of type 5 capsular polysaccharide expression by *Staphylococcus aureus*. Journal of Bacteriology 176: 4883-4889.
31. Loir YL, Baron F, Gautier M (2003). *Staphylococcus aureus* and food poisoning. Genetics & Molecular Research 2: 63-76.
32. Ming TH, Geng L, Feng Y, Lu C, Zhou J, Li Y, Zhang D, He S, Li Y, Cheong L, Su X (2019). iTRAQ-based quantitative proteomic profiling of *Staphylococcus aureus* under different osmotic stress conditions. Frontiers in Microbiology 10: 1082.
33. Ming TH, Han JJ, Li YY, Lu CY, Qiu D, Li Y, Zhou J, Su XR. (2018). A metabolomics and proteomics study of the *Lactobacillus plantarum* in the grass carp fermentation. BMC Microbiology 18: 216.
34. Nagayama K, Fujita K, Takashima Y, Ardin AC, Ooshima T, Matsumoto NM (2014). Role of ABC transporter proteins in stress responses of *Streptococcus* mutans. Oral Health & Dental Management 13: 359-365.

35. Oshima T, Aiba H, Masuda Y, Kanaya S, Sugiura M, Wanner BL, Mori H, Mizuno T (2002). Transcriptome analysis of all two-component regulatory system mutants of *Escherichia coli* K-12. Molecular Microbiology 46: 281-291.
36. Price WA, Poon CK, Benson MA, Eidem TT, Roux CM, Boyd JM, Dunman PM, Torres VJ, Krulwich, TA (2013). Transcriptional profiling of *Staphylococcus aureus* During growth in 2 M NaCl leads to clarification of physiological roles for Kdp and Ktr K^+ uptake systems. mBio 4: e00407-00413.
37. Raboy V, Gerbasi P (1996). Genetics of myo-inositol phosphate synthesis and accumulation. Sub-cellular biochemistry 26: 257-285.
38. Ran S, Liu B, Jiang W, Sun Z, Liang J. (2015). Transcriptome analysis of *Enterococcus faecalis* in response to alkaline stress. Frontiers in Microbiology 6: 795.
39. Ran S, Liu B, Jiang W, Sun Z, Liang J (2015b). Transcriptome analysis of *Enterococcus faecalis* in response to alkaline stress. Frontiers in Microbiology 6: 795.
40. Rigali S, Derouaux A, Giannotta F, Dusart J. (2002). Subdivision of the helix-turn-helix GntR family of bacterial regulators in the FadR, HutC, MocR, and YtrA subfamilies. Journal of Biological Chemistry 277: 12507-12515.
41. Rodriguez MC, Riesco PF, Garcia FC, Alonso CC, Capita R (2019). Susceptibility of *Listeria monocytogenes* planktonic cultures and biofilms to sodium hypochlorite and benzalkonium chloride. Food Microbiology 82: 533-540.
42. Schuster CF, Bellows LE, Tosi T, Campeotto I, Corrigan RM, Freemont P, Gründling A (2016). The second messenger c-di-AMP inhibits the osmolyte uptake system OpuC in *Staphylococcus aureus*. Science Signaling 9: ra81.
43. Sergelidis D, Abrahim A, Papadopoulos T, Soultos N, Martziou E, Koulourida V, Govaris A, Pexara A, Zdragas A, Papa A (2014). Isolation of methicillin-resistant *Staphylococcus spp*. from ready-to-eat fish products. Letters in Applied Microbiology 59: 500-506.
44. Zhang S, Yang W, Zhao Q, Zhou X, Jiang L, Ma S, Liu X, Li Y, Zhang C, Fan Y, Chen R. Analysis of weighted co-regulatory networks in maize provides insights into new genes and regulatory mechanisms related to inositol phosphate metabolism. BMC Genomics 17: 129.
45. Vijaranakul U, Nadakavukaren MJ, De Jonge BL, Wilkinson BJ, Jayaswal RK (1995). Increased cell size and shortened peptidoglycan interpeptide bridge of NaCl-stressed *Staphylococcus aureus* and their reversal by glycine betaine. Journal of Bacteriology 177: 5116-5121.
46. Vilhelmsson O, Miller KJ (2002). Synthesis of pyruvate dehydrogenase in *Staphylococcus aureus* is stimulated by osmotic stress. Applied & Environmental Microbiology 68: 2353-2358.
47. Wei K, Tang DJ, He YQ, Feng JX, Jiang BL, Lu GT, Chen B, Tang JL (2007). hpaR, a putative marR family transcriptional regulator, is positively controlled by HrpG and HrpX and involved in the pathogenesis, hypersensitive response, and extracellular protease production of *Xanthomonas campestris* pathovar campestris. Journal of Bacteriology 189: 2055-2062.
48. Wong TW, Liao SZ, Ko WC, Wu CJ, Wu SB, Chuang YC, Huang IH (2019). Indocyanine green-mediated photodynamic therapy reduces methicillin-resistant *Staphylococcus aureus* Drug resistance. Journal

of Clinical Medicine 8: 411.

49. Xin W, Zhang L, Zhang W, Gao J, Yi J, Zhen X, Li Z, Zhao Y, Peng C, Zhao C (2019). An integrated analysis of the rice transcriptome and metabolome reveals differential regulation of carbon and nitrogen metabolism in response to nitrogen availability. International Journal of Molecular Sciences 20: 2349.
50. Xu Z, Xie J, Soteyome T, Peters BM, Shirtliff ME, Liu J, Harro JM (2019). Polymicrobial interaction and biofilms between *Staphylococcus aureus* and *Pseudomonas aeruginosa*: an underestimated concern in food safety. Current Opinion in Food Science 26: 57-64.
51. Yin W, Wang Y, Liu L, He J (2019). Biofilms: The Microbial "Protective Clothing" in Extreme Environments. International journal of molecular sciences 20: 3423.
52. Zhang X, Wen H, Wang H, Ren Y, Zhao J, Li Y (2017). RNA-Seq analysis of salinity stress-responsive transcriptome in the liver of spotted sea bass (*Lateolabrax maculatus*). PLOS ONE 12: e0173238.
53. Zhao X, Liu Z, Liu Z, Meng R, Shi C, Chen X, Bu X, Guo N (2018). Phenotype and RNA-seq-Based transcriptome profiling of *Staphylococcus aureus* biofilms in response to tea tree oil. Microbial Pathogenesis 123: 304-313.

Figures

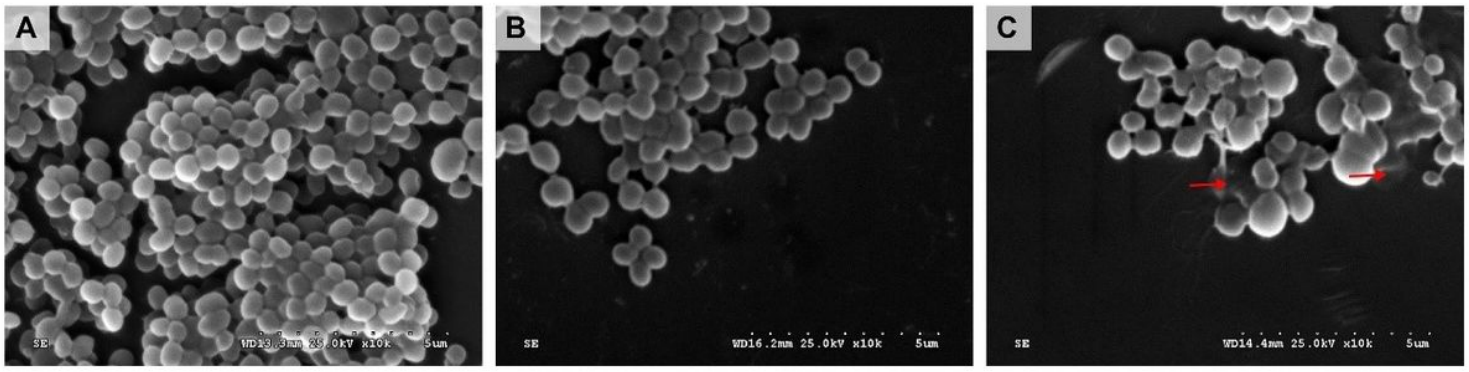

Figure 1

Morphology of S. aureusZS01 under SEM. (A) 0% NaCl group; (B) 10% NaCl group; (C) 20% NaCl group. SEM images of NaCl treated and untreated S. aureus ZS01cells. S. aureus ZS01 was incubated for 48 hours in a broth medium supplemented with 0%, 10% and 20% NaCl, respectively. ×10K-fold. Red solid arrows have indicated major structural changes.

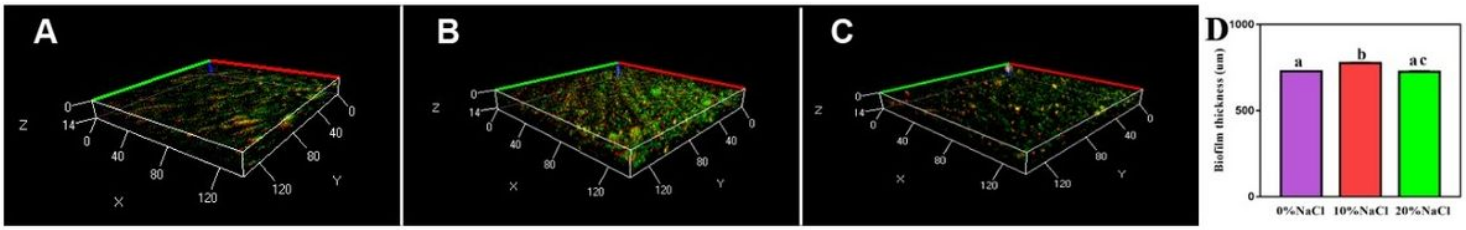

Figure 2

CLSM images of S. aureus ZS01 biofilm formation changes. (A) 0% NaCl group; (B) 10% NaCl group; (C) 20% NaCl group; (D) The thickness of biofilm. S. aureus ZS01 was incubated for 48 hours in a broth medium supplemented with 0%, 10% and 20% NaCl, respectively. The concentration of the collected bacterial solution is 5×106 CFU/mL. Biofilm was stained with FITC-ConA (4°C, 30min) and PI (4°C, 15min), then imaged. λex=488nm, λem=520nm was used for FITC-ConA detection (green channel), λex= 543nm , λem=572nm was used for PI detection (red channel). Three fields of view are randomly selected for each specimen and scanned layer by layer along the Z axis. CLSM images were captured using a Zeiss LSM880 confocal laser scanning microscope (Zeiss LSM880, Germany) with ×40 objective lens. Z stack represents the thickness of biofilm.

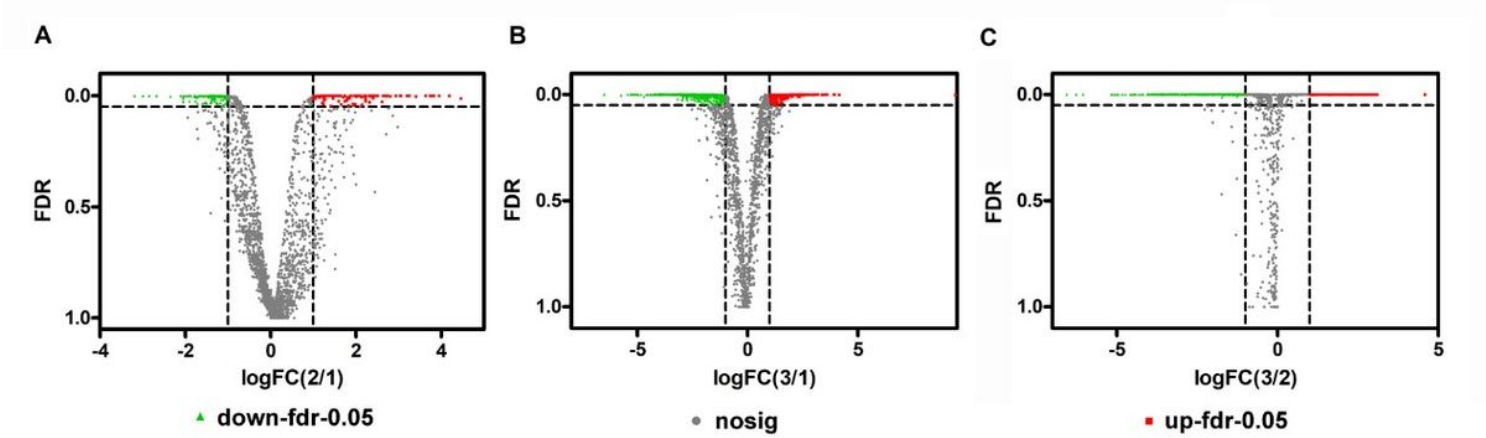

Figure 3

Volcano plot of the genes identified in S. aureus ZS01 treated with different concentrations of NaCl. (A) 0% NaCl vs 10% NaCl; (B) 0% NaCl vs 20% NaCl; (C) 10% NaCl vs 20% NaCl. Each point represents a gene, and the red and green areas represents upregulated (Log2FC ≥ 1 and FDR ≤ 0.05) and downregulated (Log2FC ≤ -1 and FDR ≤ 0.05) genes, respectively.

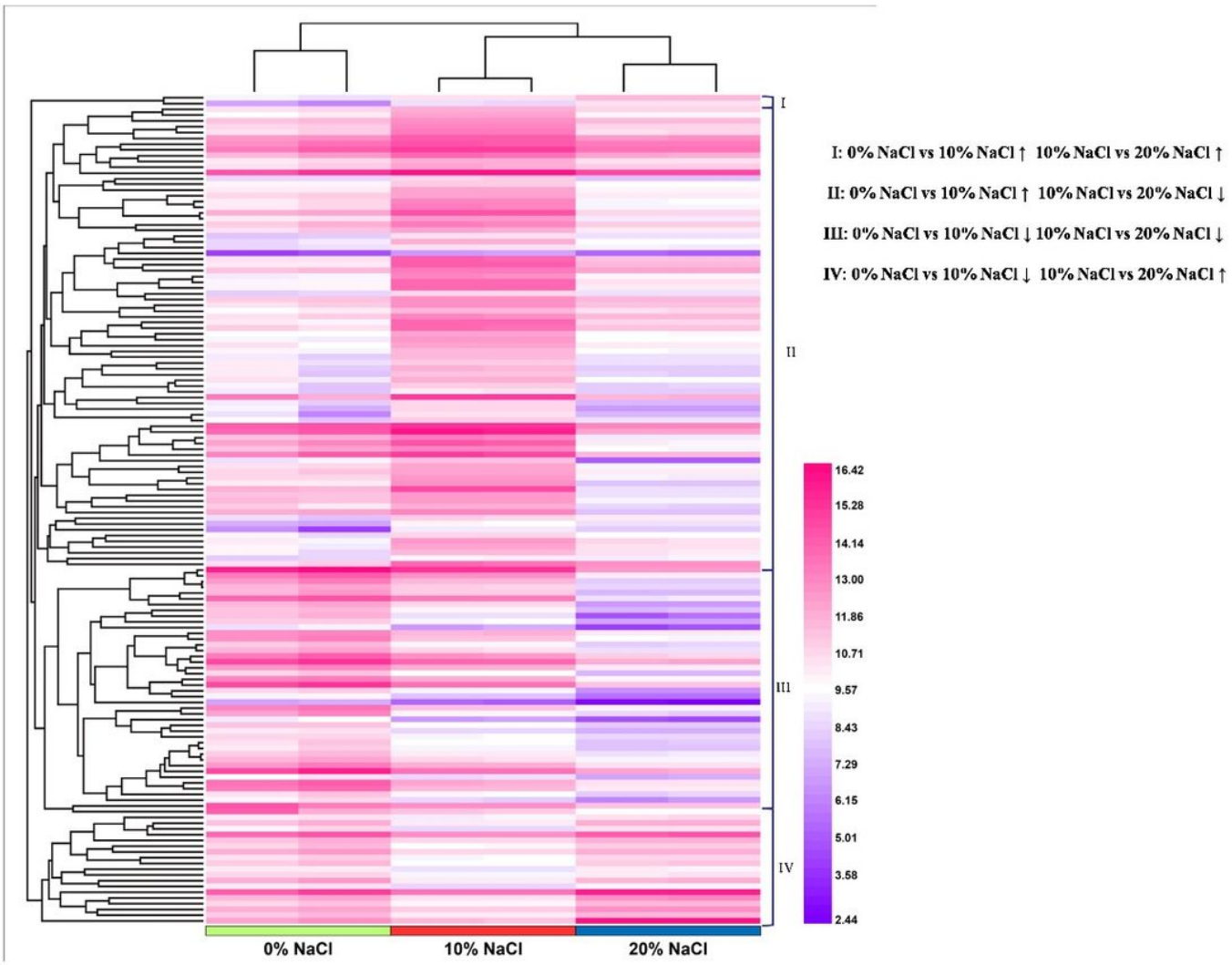

Figure 4

Functional clustering analysis of the DEGs with increasing NaCl concentrations. Pattern I (increase/increase): genes that were stepwise upregulated with increasing NaCl concentrations; Pattern II (increase/decrease): genes that reached their highest expression levels in the 10% NaCl group; Pattern III (decrease/decrease): genes that were stepwise downregulated with increasing NaCl concentrations and Pattern IV (decrease/increase): genes that reached their lowest expression levels in the 10% NaCl group.

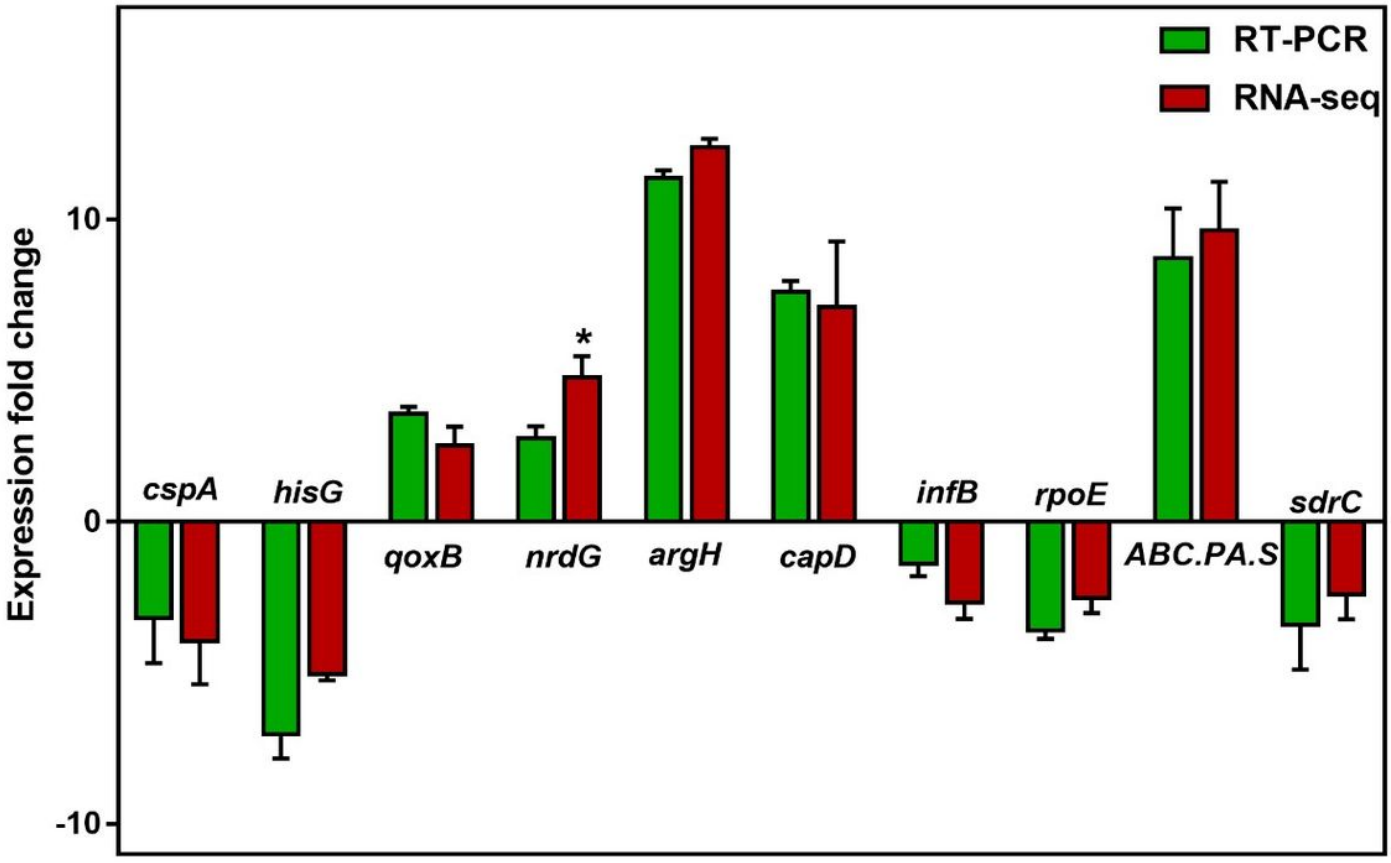

Figure 5

Experimental validation of DEGs by qRT-PCR assays. Candidate genes mainly included cold shock protein gene (cspA), ATP phosphoribosyltransferase gene (hisG), quinol oxidase subunit 1 gene (qoxB), anaerobic ribonucleotide reductase small subunit gene (nrdG), argininosuccinate lyase (argH), capsular polysaccharide synthesis enzyme gene (capD), translation initiation factor (IF)-2 gene (infB), DNA-directed RNA polymerase subunit delta gene (rpoE), glutamate ABC transporter permease gene (ABC.PA.S), serine-aspartate repeat protein F gene (sdrC). The expression of the fold change in the Y-axis indicates the ratios of DEGs (red bar) or mRNA level (green bar).

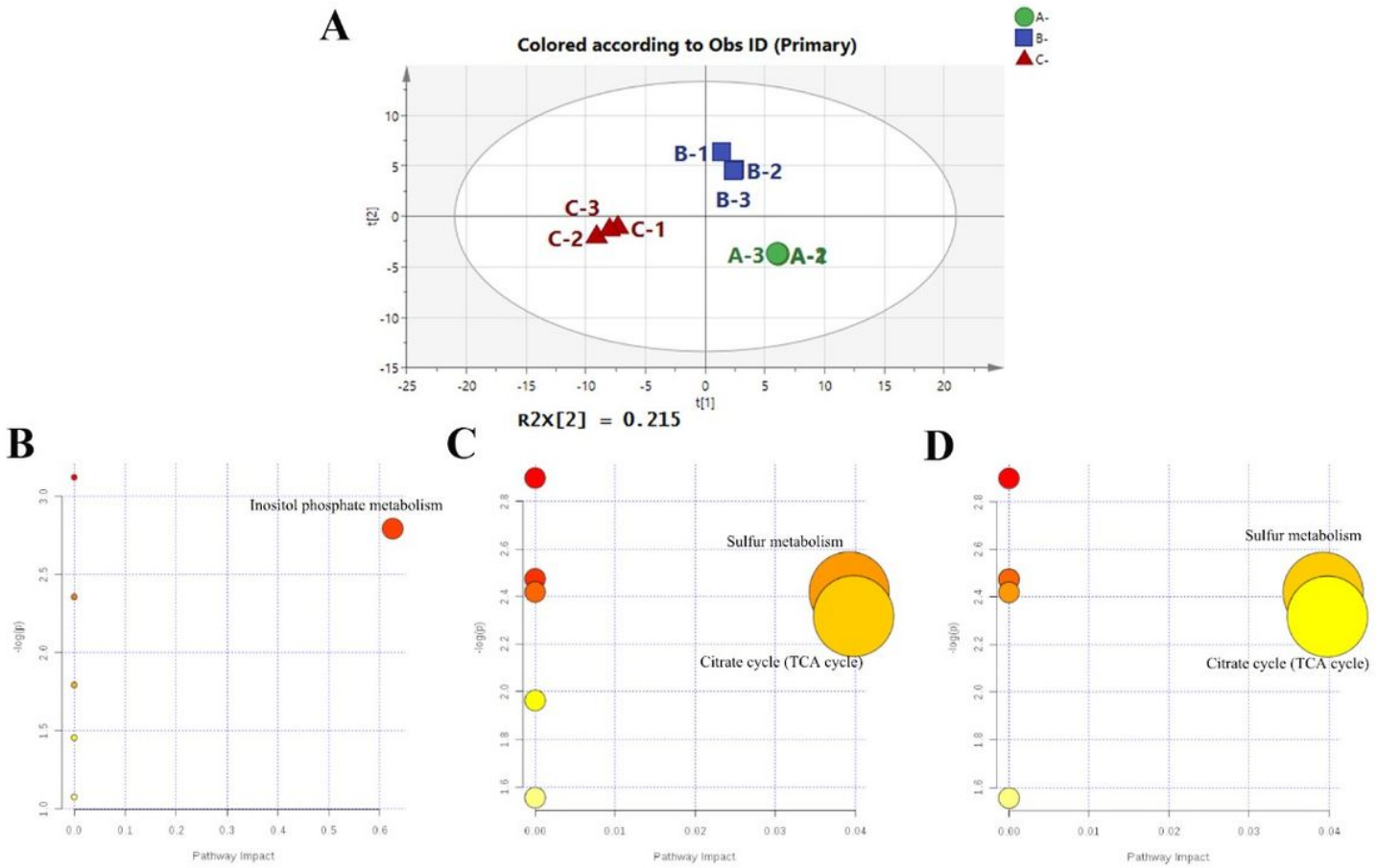

Figure 6

Score plot of principal components analysis (PCA) and pathway analysis for the biomarkers. (A) Score plot of PCA of the 0% NaCl group (green circle), 10% NaCl (blue square) and 20% NaCl group (red triangle). The t[1] and t[2] values represent the scores of each metabolite sample in the principal components 1 and 2, respectively. The ellipse indicates the 95% confidence border. Separation among different samples can be seen. (B) Bubble plot of significant metabolic pathways (0% NaCl vs 10% NaCl); (C) Bubble plot of significant metabolic pathways (10% NaCl vs 20% NaCl); (D) Bubble plot of significant metabolic pathways (0% NaCl vs 20% NaCl). According to the path enrichment analysis and pathway impact values, the matched pathway is displayed. Circles represent matched metabolic pathways, which were retrieved from KEGG. The color intensity indicates the significance of the pathway, while size indicates the pathway impact score (the centrality of its involved metabolites). The bigger the value of -log10(P), the more this pathway is disturbed. The bigger the value of impact, the more this pathway is disturbed.

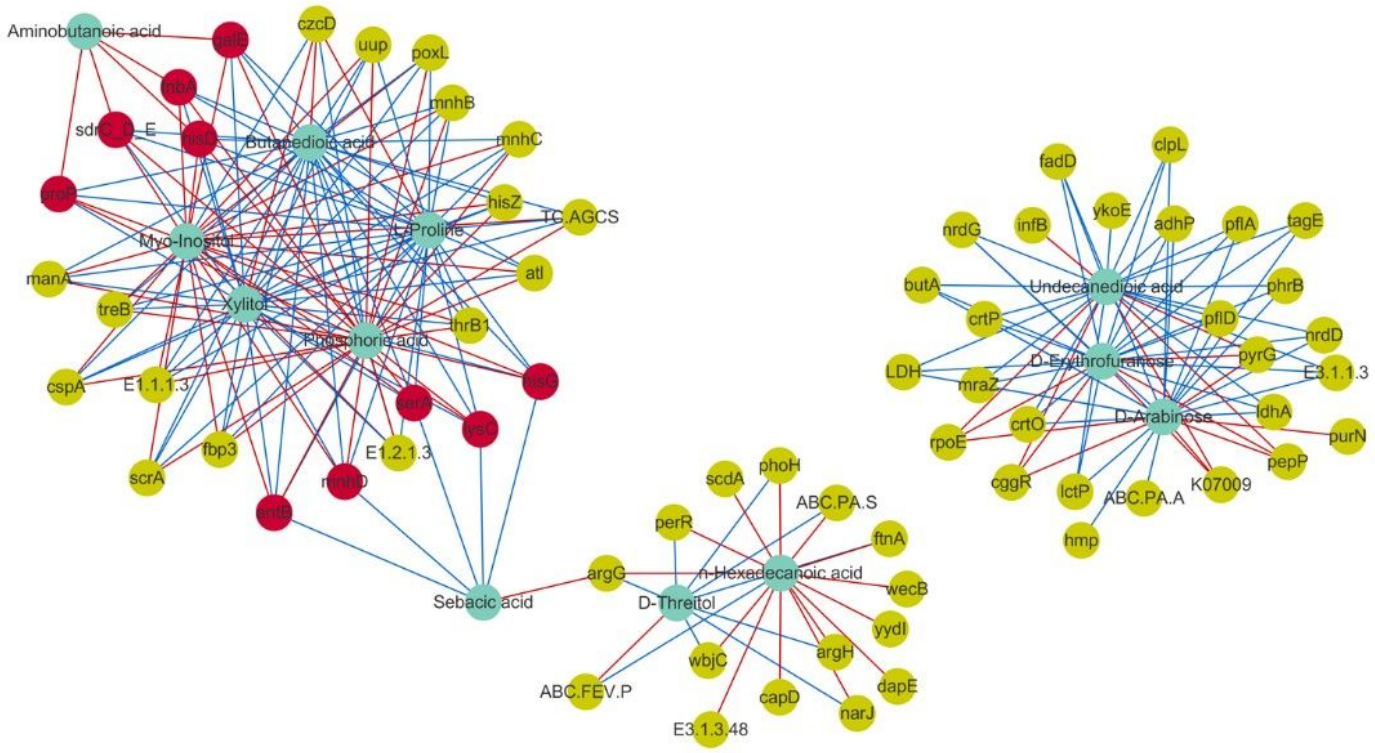

Figure 7

Integrated Analysis of Transcriptome and Metabolome. The Spearman correlation network reveals the regulatory mechanisms of the salinity stress response mechanisms. Results of the correlation analysis between key candidate genes and discriminant metabolites. Different colors of nodes represent metabolites (blue), genes (yellow), and hub genes (red). Positive correlations are indicated by a red line, and negative correlations are indicated by a green line. The thickness of the line represents the magnitude of the correlation coefficient.

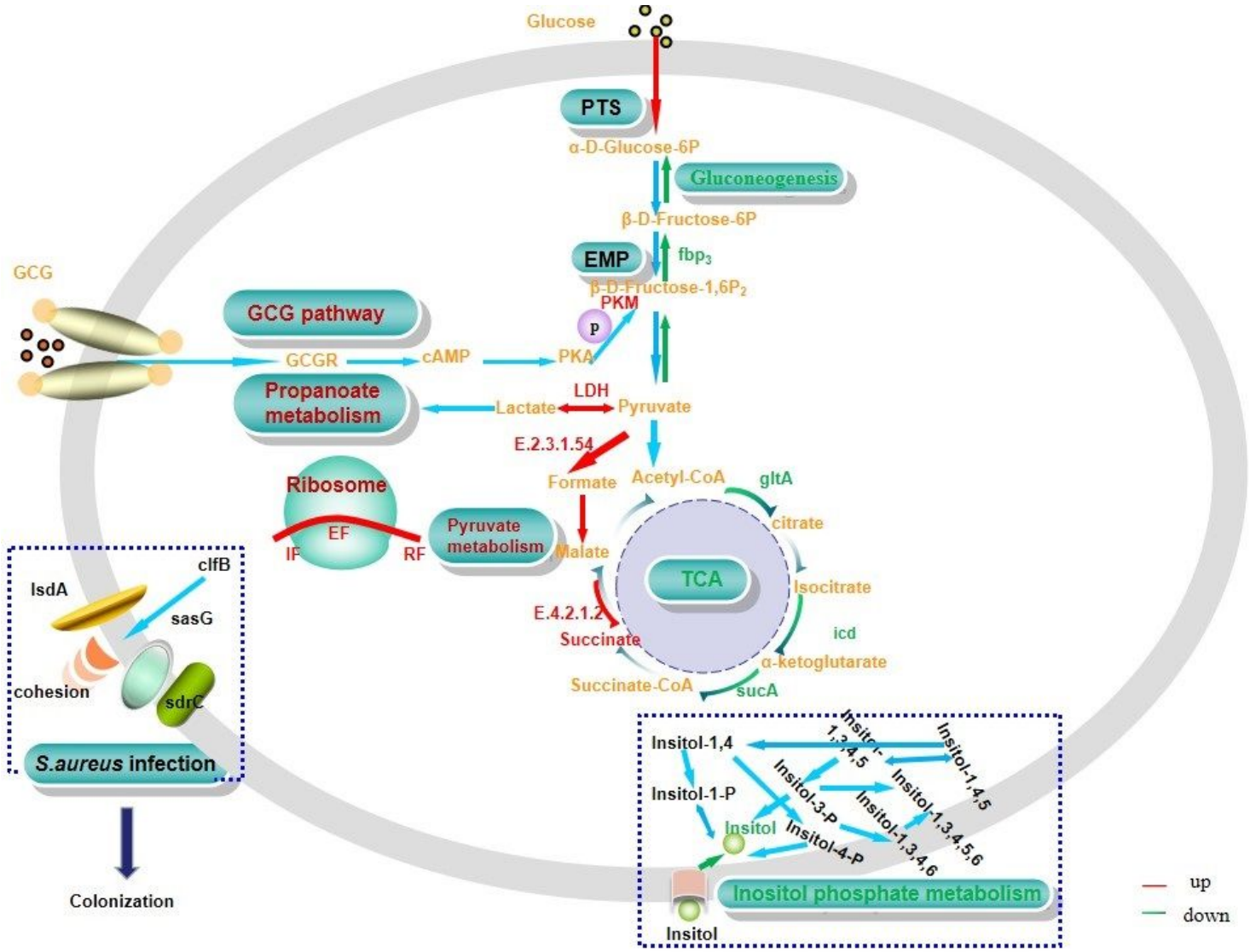

Figure 8

Relevant metabolic pathways in S. aureus ZS01. Red font indicates upregulated genes, and green font indicates downregulated genes. Matched genes include fructose-1,6-bisphosphatase (fbp3), fumarate hydratase (E4.2.1.2), formate acetyltransferase (E2.3.1.54), citrate synthase (gltA), isocitrate dehydrogenase (icd) and 2-oxoglutarate dehydrogenase E1 component (sucA). IF means initiation factor, EF means elongation factor, RF means release factor.

Supplementary Files

This is a list of supplementary files associated with this preprint. Click to download.

- SupplementaryMaterial.rar